Mode Reduction for Efficient Modeling of Photonic Crystal Slab Structures

Lijun Yuan and Ya Yan Lu

***Abstract*—Rigorous numerical simulations for photonic crystal (PhC) slab structures and devices are difficult due to the complicated three-dimensional geometry, high index-contrast, sharp edges, and possibly inhomogeneity at infinity. The approach based on expanding the field in one-dimensional vertical modes has great potential, but is currently limited by the relatively large number of modes needed for maintaining the accuracy of the solutions. In this paper, we show that if a single hole is first analyzed with the full set of vertical modes, the number of modes can be reduced to less than one third of the total in the main part of the computation. This leads to a speedup of more than 27 times. The method is illustrated by computing the transmission and reflection spectra for a PhC slab with a finite number of hole arrays.**

I. Introduction

PHOTONIC crystals have attracted much attention in recent years due to their interesting properties such as the bandgaps and unusual dispersion effects [1]. Realistic photonic crystal (PhC) devices are usually fabricated on PhC slabs which are layered structures with a biperiodic pattern (typically a triangular lattice of air holes) perpendicular to the layers. To design and optimize PhC slab devices for practical applications, large scale numerical simulations must be performed and efficient numerical methods are needed. Existing methods such as the finite-difference domain-domain (FDTD) method [2] and the frequency-domain finite element method (FEM) [3] are widely used, but their efficiencies may be limited by the large index-contrast, sharp edges and complex geometry of the devices. In particular, FDTD requires a small grid size to resolve material interfaces and a small time step to maintain numerical stability, and FEM requires efficient iterative methods for solving the resulting large linear systems.

For linear problems in the frequency domain, it is possible to develop more efficient computational methods by taking advantage of the geometric features of the PhC devices. For PhC slab structures involving circular holes, Boscolo and Midrio [4] developed a method based on expanding the field in one-dimensional (1D) vertical modes and horizontal cylindrical waves, where the slab is assumed to be parallel to the horizontal plane. Their method is applicable to slab structures with a finite number of holes and was further enhanced by Pissoort *et al.* [5]. In a related work [6], we developed a method based on vertical mode expansions and the so-called Dirichlet-to-Neumann (DtN) maps for slabs with infinite and periodic arrays of holes. The DtN-map method can be used to take advantage of the periodicity or partial periodicity of PhC devices (i.e., the existence of many identical unit cells), and it is highly efficient for idealized two-dimensional (2D) PhC structures that have one invariant spatial direction [7]–[10]. However, these methods based on expansions in vertical modes [4]–[6] are still too expensive for simulating practical PhC slab devices, since many vertical modes are needed to reach the desired level of accuracy.

The vertical mode expansion method for PhC slab structures is closely related to the mode-matching method (also called eigenmode expansion method or modal method) for modeling piecewise uniform waveguides [11]–[20] and diffraction gratings [21]–[31]. In the mode-matching or modal method for waveguides and gratings, a main propagation direction (the direction along the waveguide axis or perpendicular to the grating surface) is first identified, the structure is divided into segments (or layers) that are invariant in that direction, the wave fields in each uniform segment are expanded in the transverse eigenmodes, and the unknown coefficients are solved from a linear system established by enforcing proper boundary conditions on the interfaces between the segments. For PhC slab devices, a main propagation direction usually does not exist, but there is still a main propagation plane, i.e., the plane of the slab. Instead of uniform segments, a 3D slab structure consists of regions where the material properties vary only in the vertical direction. Therefore, it is possible to expand the electromagnetic field in each region in 1D vertical modes.

Since the computation effort of the vertical mode expansion method depends cubically on the number of modes, it is highly desirable to use less modes. However, a large number of modes may be needed to accurately enforce the boundary conditions on the interfaces between the regions. Furthermore, since the vertical direction (perpendicular to the slab) is originally unbounded and only truncated by perfectly matched layers (PMLs) [32]–[35], many modes are still needed to model the continuum of radiation modes. It appears difficult to implement the vertical mode expansion method with a significantly reduced number of modes without sacrificing the

This work was partially supported by the National Natural Science Foundation of China (project No. 11201508 and 11101453), the Scientific Research Foundation of Chongqing Technology and Business University (project No. 20125605), the Scientific and Technological Research Program of Chongqing Municipal Education Commission (grant No. KJ130726), and by the Research Grants Council of Hong Kong Special Administrative Region, China (Project No. CityU 102411).

L. Yuan is with the College of Mathematics and Statistics, Chongqing Technology and Business University, Chongqing 400067, China (e-mail: yuanlijun.ma@gmail.com).

Y. Y. Lu is with the Department of Mathematics, City University of Hong Kong, Kowloon, Hong Kong (e-mail: mayylu@cityu.edu.hk).

accuracy.

Our approach is to reduce the number of modes only after the scattering properties of a single hole are computed using the full set of eigenmodes. This is useful since the entire structure is far more difficult to analyze than a single hole. A slab with a single hole is easy to analyze, since there is a rotational symmetry. On the other hand, a slab with more than one holes no longer has the rotational symmetry, and is far more difficult to study. We consider a PhC slab with a finite number of linear hole arrays where each linear array is a periodic and infinite row of circular holes. The vertical direction is truncated by PMLs and discretized, so that the vertical modes are approximated by a finite number of numerical eigenmodes. In the first stage, we use all numerical modes to study the scattering properties of a single hole. Based on that, we reduce the number of modes and study the hole arrays in the second stage. We found that the accuracy is acceptable if one-third of the total number of numerical eigenmodes are retained. In that case, we obtain a speedup of 27 times.

II. Vertical Mode Expansions

Due to the many practical applications of PhC slabs, it is important to study the scattering of light by holes in a slab. We consider a finite number of linear hole arrays in a slab, where each linear array is infinite and periodic, and the centers of the holes are located on a triangular lattice. In Fig. 1(a) we

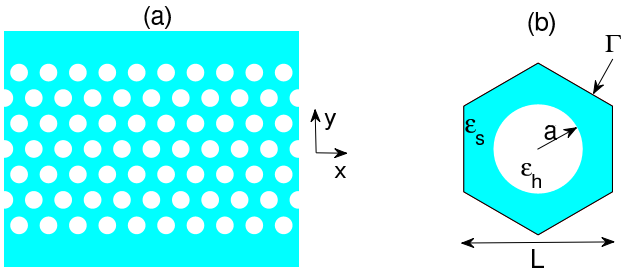

Fig. 1. (a): Top view of a photonic crystal slab with seven hole arrays; (b): Cross section Ω_0 of a hexagon unit cell Ω.

show the top view of a slab with seven linear hole arrays. Since the slab has a finite thickness, the structure is three dimensional, and it must be analyzed using the full set of Maxwell's equations. In the frequency domain, these equations are

$$\nabla \times \boldsymbol{E} = ik_0\mu\boldsymbol{H}, \quad \nabla \times \boldsymbol{H} = -ik_0\varepsilon\boldsymbol{E}, \tag{1}$$

where $\boldsymbol{E}$ is the electric field, $\boldsymbol{H}$ is the magnetic field multiplied by the free space impedance, k_0 is the free space wavenumber, μ is the relative magnetic permeability, ε is the dielectric function, and the time dependence is assumed to be $e^{-i\omega t}$ for an angular frequency ω. The slab without holes is a simple waveguide with some propagating modes. Our problem is to calculate the transmitted and reflected waves, as well as the out-of-plane radiation loss, for a given incident wave which is usually a propagating mode of the slab.

Assuming the slab is parallel to the horizontal xy plane, the structure has only two distinct vertical profiles. That is, $\varepsilon = \varepsilon_s(z)$ and $\mu = \mu_s(z)$ in the slab region, and $\varepsilon = \varepsilon_h(z)$ and $\mu = \mu_h(z)$ in the hole region. The electromagnetic field in these two regions can be expanded in the 1D modes corresponding to the respective vertical profiles. To avoid the continuous spectra, the z variable can be truncated by PMLs [32]–[35]. If z is truncated to (z_0, z_*), then the vertical modes in the slab region satisfy

$$\frac{\rho_s}{S}\frac{d}{dz}\left[\frac{1}{S\rho_s}\frac{d\phi_s^{(p)}}{dz}\right] + k_0^2\varepsilon_s\mu_s\phi_s^{(p)} = [\eta_s^{(p)}]^2\phi_s^{(p)} \tag{2}$$

for $z_0 < z < z_*$, where $p = 1$ and $\rho_s = \mu_s$ for the transverse electric (TE) polarization, $p = 2$ and $\rho_s = \varepsilon_s$ for the transverse magnetic (TM) polarization, and $S = S(z)$ is a complex function related to the PMLs ($S \neq 1$ only in the PMLs). Furthermore, we assume the boundary conditions are

$$\phi_s^{(1)} = 0, \quad \frac{d\phi_s^{(2)}}{dz} = 0 \quad \text{at} \quad z = z_0,\ z_*, \tag{3}$$

then the eigenvalue problems (2) and (3) have infinite sequence of eigenpairs. We denote them as $\phi_{s,j}^{(p)}(z)$ and $\eta_{s,j}^{(p)}$ for $j = 1$, 2, 3, ...

In the slab region, since ε_s and μ_s depend only on z, it can be proved that H_z and E_z satisfy separate 3D Helmholtz equations, and they can be expanded in the vertical TE and TM modes respectively as follows:

$$H_z(x,y,z) = \frac{1}{\mu_s(z)}\sum_{j=1}^{\infty}\phi_{s,j}^{(1)}(z)\,V_{s,j}^{(1)}(x,y), \tag{4}$$

$$E_z(x,y,z) = \frac{1}{\varepsilon_s(z)}\sum_{j=1}^{\infty}\phi_{s,j}^{(2)}(z)\,V_{s,j}^{(2)}(x,y), \tag{5}$$

where $V_{s,j}^{(p)}$ satisfies the following 2D Helmholtz equation

$$\frac{\partial^2 V_{s,j}^{(p)}}{\partial x^2} + \frac{\partial^2 V_{s,j}^{(p)}}{\partial y^2} + [\eta_{s,j}^{(p)}]^2\,V_{s,j}^{(p)} = 0. \tag{6}$$

The derivation of (4), (5) and (6) can be found in earlier works [4], [6]. The other components of the electromagnetic field are related to H_z and E_z. In the hole region, there are similar TE and TM modes, and similar expansions for H_z and E_z. We only need to change the subscript from "s" to "h".

For a slab with a single circular hole, we use the cylindrical coordinate system $\{r, \theta, z\}$ such that the z axis is the axis of the cylindrical hole, then the field inside and outside the hole can be further expanded in horizontal cylindrical waves. We have

$$V_{h,j}^{(p)}(x,y) = \sum_{m=-\infty}^{\infty} c_{jm}^{(p)} J_m(\eta_{h,j}^{(p)} r)\, e^{im\theta}, \quad r < a, \tag{7}$$

$$V_{s,j}^{(p)}(x,y) = \sum_{m=-\infty}^{\infty}\Big[a_{jm}^{(p)} J_m(\eta_{s,j}^{(p)} r) \tag{8}$$

$$+ b_{jm}^{(p)} H_m^{(1)}(\eta_{s,j}^{(p)} r)\Big]\, e^{im\theta}, \quad r > a, \tag{9}$$

where J_m is a Bessel function and $H_m^{(1)}$ is a Hankel function of the first kind. The terms with the coefficients $\{a_{jm}^{(p)}\}$, $\{b_{jm}^{(p)}\}$ and $\{c_{jm}^{(p)}\}$ correspond to the incident wave impinging upon the hole, the scattered wave outside the hole and the wave

transmitted into the hole, respectively. For given $\{a_{jm}^{(p)}\}$, the coefficients $\{b_{jm}^{(p)}\}$ and $\{c_{jm}^{(p)}\}$ can be solved. Due to the rotational symmetry, there is no coupling for different values of m, i.e., for different Fourier modes. On the other hand, the vertical modes including both TE and TM modes, are coupled together. Matching H_z, E_z, H_θ and E_θ (the θ components of the electromagnetic field) on the interface between the slab and hole regions, i.e., at $r = a$, we can find matrices $\mathbf{D}_m$ and $\mathbf{C}_m$ for each m [4], such that

$$\begin{bmatrix} \boldsymbol{b}_m^{(1)} \\ \boldsymbol{b}_m^{(2)} \end{bmatrix} = \mathbf{D}_m \begin{bmatrix} \boldsymbol{a}_m^{(1)} \\ \boldsymbol{a}_m^{(2)} \end{bmatrix}, \quad \begin{bmatrix} \boldsymbol{c}_m^{(1)} \\ \boldsymbol{c}_m^{(2)} \end{bmatrix} = \mathbf{C}_m \begin{bmatrix} \boldsymbol{a}_m^{(1)} \\ \boldsymbol{a}_m^{(2)} \end{bmatrix}, \tag{10}$$

where $\boldsymbol{a}_m^{(p)}$, $\boldsymbol{b}_m^{(p)}$ and $\boldsymbol{c}_m^{(p)}$ are column vectors for $\{a_{jm}^{(p)},\, j = 1, 2, ...\}$, $\{b_{jm}^{(p)},\, j = 1, 2, ...\}$ and $\{c_{jm}^{(p)},\, j = 1, 2, ...\}$, respectively.

Many different implementations of the vertical mode expansion method are possible, and they correspond to different ways for computing the eigenmodes and enforcing the boundary conditions on the interfaces. If ε and μ are piecewise constant in z, the eigenvalue problems (2) and (3) can be solved analytically, in the sense that the eigenfunctions are given analytically, but the eigenvalues are solved numerically as the zeros of a transcendental function. This approach is not so convenient, since it is not easy to systematically find zeros in the complex plane, and it is not clear how to choose finite number of modes to truncate the expansions. On the other hand, it is very simple to solve the 1D eigenvalue problems by a numerical method. We use a fourth order finite difference method with a staggered grid [6]. The TE and TM eigenvalue problems are approximated by matrix eigenvalue problems involving $N_1 \times N_1$ and $N_2 \times N_2$ matrices, respectively, where $N_2 = N_1 + 1$. Furthermore, we enforce the boundary conditions at $r = a$ by simply matching the four field components at all discretization points of z. As a result, the matrices $\mathbf{D}_m$ and $\mathbf{C}_m$ can be computed in $O(N^3)$ operations where $N = N_1 + N_2$. If we keep M Fourier modes (by truncating m to $-M/2 \le m < M/2$ if M is even), then the scattering problem of a single hole in a slab can be solved using $O(MN^3)$ operations.

III. DtN-map method

For a slab with a finite number of hole arrays, we developed a computational method based on vertical mode expansions and DtN maps [6]. Since the centers of the holes lie on a triangular lattice, we may consider hexagon unit cells with a hole at the center. The horizontal cross section Ω_0 of a unit cell Ω is shown in Fig. 1(b). The DtN map of unit cell Ω is an operator that maps H_z and E_z to their normal derivatives on the vertical boundary of Ω. In connection with vertical mode expansions (4), we can define a more practical DtN map as the operator $\tilde{\Lambda}$ satisfying

$$\tilde{\Lambda} \begin{bmatrix} \boldsymbol{V}_s^{(1)} \\ \boldsymbol{V}_s^{(2)} \end{bmatrix} = \frac{\partial}{\partial \nu} \begin{bmatrix} \boldsymbol{V}_s^{(1)} \\ \boldsymbol{V}_s^{(2)} \end{bmatrix} \quad \text{on} \quad \Gamma, \tag{11}$$

where Γ is the boundary of Ω_0, ∂_ν is the normal derivative operator on Γ, $\boldsymbol{V}_s^{(p)}$ is a column vector for $\{V_{s,j}^{(p)},\ j = 1, 2, ...\}$. The DtN map $\tilde{\Lambda}$ can be used to compute the reflected and transmitted waves for a given incident wave impinging on the hole arrays. The procedure is given in [6] and it is an extension of the method first developed for pure 2D problems in [36].

In practice, the DtN map $\tilde{\Lambda}$ is approximated by a matrix. When Γ is discretized by M points, $V_{s,j}^{(p)}$ becomes a column vector of length M. If we keep a total of N modes, then $\tilde{\Lambda}$ becomes an $(MN) \times (MN)$ matrix. To calculate $\tilde{\Lambda}$, we consider the solution (4) and (8) again, but now keep M Fourier terms and consider the coefficients $\{a_{jm}^{(p)}\}$ as arbitrary. Evaluating this general solution at the M points on Γ, we get a linear relation between $V_{s,j}^{(p)}$ and $\{a_{jm}^{(p)}\}$. We can also write down $\partial_\nu V_{s,j}^{(p)}$ analytically, then evaluate them at the M points on Γ, and get a linear relation between $\partial_\nu V_{s,j}^{(p)}$ and $\{a_{jm}^{(p)}\}$. The DtN map $\tilde{\Lambda}$ is obtained by eliminating $\{a_{jm}^{(p)}\}$. This process requires $O(M^3N^3)$ operations. Due to the cubic dependence on M, it is far more difficult to analyze hole arrays than a single hole.

IV. Mode reduction

To speed up the DtN-map method for analyzing PhC slab structures, we develop a mode reduction technique to construct approximate DtN maps for the unit cells. The procedure depends on the incident wave for the problem being considered. For hole arrays in a slab, the incident wave is usually the fundamental TE or TM mode with a plane wave behavior in the horizontal plane. If the incident wave is the first TE mode with the vertical profile $\phi_{s,1}^{(1)}(z)$, we can find the most relevant vertical modes by analyzing the scattering problem of a single hole with two cylindrical incident waves $\phi_{s,1}^{(1)}(z) J_m(\eta_{s,1}^{(1)} r) e^{im\theta}$ for $m = 0$ and 1.

Assuming the vertical modes in the slab region are normalized by

$$\int_{z_0}^{z_*} \rho_s^{-1}(z) S(z) [\phi_{s,j}^{(p)}(z)]^2 \, dz = 1,$$

the cylindrical incident wave above gives rise to a scattered wave as the second term in (8), where the coefficients $\{b_{jm}^{(p)}\}$ are given as the first column of matrix $\mathbf{D}_m$. That column consists of two parts $\boldsymbol{f}_m$ and $\boldsymbol{g}_m$ with N_1 and N_2 elements, respectively, and they are the coefficients of the TE and TM vertical modes in the scattered wave. We select the TE modes based on the magnitudes of the elements in $\boldsymbol{f}_0$ and $\boldsymbol{f}_1$. More precisely, for an integer $\tilde{N}_1 < N_1$, we choose $\tilde{N}_1$ elements with the largest magnitude in $\boldsymbol{f}_0$ and $\boldsymbol{f}_1$, respectively, and find the mode indices for all these elements, and finally get N_1^* TE modes that we need to keep. Similarly, we find N_2^* TM modes from the two vectors $\boldsymbol{g}_0$ and $\boldsymbol{g}_1$. Based on the total $N_* = N_1^* + N_2^*$ selected modes, we can find an $(MN_*) \times (MN_*)$ matrix approximating the DtN map. The required number of operations is $O(M^3 N_*^3)$.

V. Numerical example

In this section, we present a numerical example to illustrate the efficiency of our mode reduction technique. We consider a dielectric slab with seven hole arrays parallel to the x axis as shown in Fig. 1(a). The centers of the holes are

lattice points of a triangular lattice with lattice constant L. The radius of the holes and thickness of the slab are $0.25L$ and $0.5L$, respectively. The dielectric constant of the slab is $\varepsilon = 11.56$, and it is surrounded by air. The incident wave is the fundamental TE mode propagating in the negative y direction, i.e.,

$$H_z^{(i)}(x,y,z) = \phi_{s,1}^{(1)}(z)e^{-i\eta_{s,1}^{(1)}y}, \quad E_z^{(i)}(x,y,z) = 0.$$

In the following calculations, the vertical direction is truncated to an interval with the total length $4.5L$. The eigenvalue problems (2) are discretized by a fourth order finite difference scheme [6] with grid size $\Delta z = 4.5L/136$. This gives rise to $N_1 = 135$ TE modes and $N_2 = 136$ TM modes (the total number of modes is $N = 271$). In the horizontal plane, we keep $M = 42$ Fourier modes in the cylindrical wave expansions, and choose the same number of sampling points on Γ. Since the structure and the incident wave are both symmetric with respect to the middle plane of the slab, only the vertical modes with the same symmetry are excited. The total of number of such modes is $N_{sym} = 136$ including 68 TE modes and 68 TM modes. Using the mode reduction technique, we are able to obtain a satisfactory accuracy with less than one third of the total modes. Fig. 2 compares the reflection and transmission spectra computed by the DtN-map method with and without the mode reduction technique. The

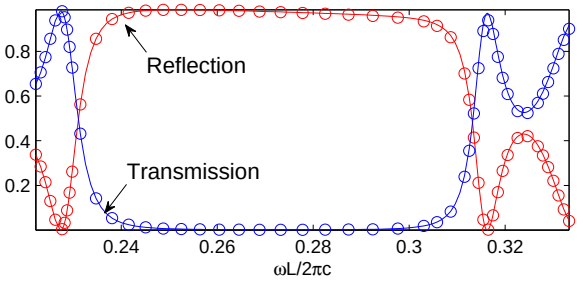

Fig. 2. Reflection and transmission spectra shown in red and blue respectively, for 7 hole arrays in a slab. The incident wave is the fundamental TE mode of the slab in normal incidence. Solid lines: solutions with all 136 vertical modes. "○": solutions with $N_* = 30$ modes.

numbers of vertical modes used are $N_* = 30$ (for 15 TE modes and 15 TM modes) and $N_{sym} = 136$, respectively. The maximum absolute error for reflection and transmission is 0.011 and 0.032, respectively. Notice that N_* is only about 23% of N_{sym}.

VI. Conclusion

A PhC slab structure or device can be quite complicated in the horizontal plane parallel to the slab, but it has only two distinct vertical profiles (in the slab and hole regions, respectively) and both are very simple. The approach based on expanding the field in vertical modes [4] may lead to efficient computational methods, but is currently limited by the relatively large number of vertical modes needed to maintain the accuracy of the solution. It appears that many of these modes are only needed to enforce the boundary conditions on the interfaces between the slab and hole regions. If the interfaces are first analyzed with the full set of modes, it is possible to have a significant reduction for the number of modes in the remaining computations.

The above idea has been realized by first analyzing the scattering properties for a single hole in a slab using the full set of vertical modes, then construct a DtN map for the unit cells using reduced number of vertical modes, and apply the DtN map for analyzing a slab with a finite number of hole arrays. The first step for the single hole requires $O(MN^3)$ operations, where N is the total number of numerical vertical modes and M is the number of retained Fourier modes. With the mode reduction technique, the required operations for the the main step is reduced from $O(M^3N^3)$ to $O(M^3N_*^3)$. Since typically $N_* < N/3$, we achieve a speedup of more than 27 times.

References

[1] D. Joannopoulos, S. G. Johnson, J. N. Winn, and R. D. Meade, "Photonic Crystals: Molding the Flow of Light," 2nd Ed., Princeton University Press, Princeton, NJ, 2008.

[2] A. Taflove and S. C. Hagness, "Computational Electrodynamics: the finite-difference time-domain method," 2nd ed., Artech House, 2000.

[3] Y. J. Li and J. M. Jin, "Fast full-wave analysis of large-scale three-dimensional photonic crystal devices," *J. Opt. Soc. Am. B*, vol. 24, pp. 2406-2415, 2007.

[4] S. Boscolo and M. Midrio, "Three-dimensional multiple-scattering technique for the analysis of photonic-crystal slabs," *J. Lightwave Technol.*, vol. 22, pp. 2778-2786, 2004.

[5] D. Pissoort, E. Michielssen, D. V. Ginste, and F. Olyslager, "Fast-multipole analysis of electromagnetic scattering by photonic crystal slabs," *J. Lightwave Technol.*, vol. 25, pp. 2847- 2863, 2007.

[6] L. Yuan and Y. Y. Lu, "Dirichlet-to-Neumann map method for analyzing hole arrays in a slab," *J. Opt. Soc. Am. B*, vol. 27, no. 12, pp. 2568-2579, 2010.

[7] Z. Hu and Y. Y. Lu, "Efficient analysis of photonic crystal devices by Dirichlet-to-Neumann maps," *Opt. Express*, vol. 16, no. 22, pp. 17383-17399, 2008.

[8] Z. Hu and Y. Y. Lu, "Improved Dirichlet-to-Neumann map method for modeling extended photonic crystal devices," *Opt. Quant. Electron.*, vol. 40, pp. 921-932, 2008.

[9] Z. Hu and Y. Y. Lu, "A simple boundary condition for terminating photonic crystal waveguides," *J. Opt. Soc. Am. B*, vol. 29, no. 6, pp. 1356-1360, 2012.

[10] L. Yuan and Y. Y. Lu, "Efficient numerical method for analyzing optical bistability in photonic crystal microcavities," *Opt. Express*, vol. 21, no. 10, pp. 11952-11964, 2013.

[11] Q. H. Liu and W. C. Chew, "Analysis of discontinuities in planar dielectric waveguides: an eigenmode propagation method," *IEEE Trans. Microwave Theory Tech.*, vol. 39, no. 3, pp. 422-430, 1991.

[12] G. Sztefka and H. P. Nolting, "Bidirectional eigenmode propagation for large refractive index steps," *IEEE Photon. Technol. Lett.*, vol. 5, pp. 554-557, 1993.

[13] J. Willems, J. Haes, and R. Baets, " The bidirectional mode expansion method for 2-dimensional waveguides – the TM case," *Opt. Quant. Electron.* vol. 27, pp. 995-1007, 1995.

[14] S. F. Helfert and R. Pregla, "Efficient analysis of periodic structures," *J. Lightwave Technol.*, vol. 16, pp. 1694-1702, 1998.

[15] P. Bienstmain and R. Baets, "Optical modelling of photonic crystals and VCSELs using eigenmode expansion and perfectly matched layers," *Opt. Quant. Electron.*, vol. 33, pp. 327-341, 2001.

[16] E. Silberstein, P. Lalanne, J. P. Hugonim, and Q. Cao, "Use of grating theories in integrated optics," *J. Opt. Soc. Am. A*, vol. 18, pp. 2865-2875, 2001.

[17] M. Hammer, "Hybrid analytical/numerical coupled-mode modeling of guided wave devices," *J. Lightwave Technol.*, vol. 25, no. 9, pp. 2287-2298, 2007.

[18] J. Čtyroký, "Improved bidirectional mode expansion propagation algorithm based on Fourier series," *J. Lightwave Technol.*, vol. 25, no. 9, pp. 2321-2330, 2007.

[19] J. Mu and W. P. Huang, "Simulation of three-dimensional waveguide discontinuities by a full-vector mode-matching method based on finite-difference schemes," *Opt. Express*, vol. 16, pp. 18152-18163, 2008.

[20] W. P. Huang, L. Han, and J. Mu, "A rigorous circuit model for simulation of large-scale photonic integrated circuits," *IEEE Photonics Journal*, vol. 4, pp. 1622-1638, 2012.

[21] L. Li, "New formulation of the Fourier modal method for crossed surface-relief gratings," *J. Opt. Soc. Am. A*, vol. 14, pp. 27582767, 1997.

[22] P. Lalanne, "Improved formulation of the coupled-wave method for two-dimensional gratings," *J. Opt. Soc. Am. A*, vol. 14, pp. 15921598, 1997.

[23] G. Granet and J. P. Plumey, "Parametric formulation of the Fourier modal method for crossed surface-relief gratings," *J. Opt. A*, vol. 4, pp. 145149, 2002.

[24] L. Li, "Fourier modal method for crossed anisotropic gratings with arbitrary permittivity and permeability tensors," *J. Opt. A*, vol. 5, pp. 345355, 2003.

[25] T. Schuster, J. Ruoff, N. Kerwien, S. Rafler, and W. Osten, "Normal vector method for convergence improvement using the RCWA for crossed gratings," *J. Opt. Soc. Am. A*, vol. 24, pp. 28802890, 2007.

[26] P. Götz, T. Schuster, K. Frenner, S. Rafler, and W. Osten, "Normal vector method for the RCWA with automated vector field generation," *Opt. Express*, vol. 16, pp. 1729517301, 2008.

[27] R. Antos, "Fourier factorization with complex polarization bases in modeling optics of discontinuous bi-periodic structures," *Opt. Express*, vol. 17, pp. 7269-7274, 2009.

[28] T. Weiss, G. Granet, N. A. Gippius, S. G. Tikhodeev, and H. Giessen, "Matched coordinates and adaptive spatial resolution in the Fourier modal method," *Opt. Express*, vol. 17, pp. 8051-8061, 2009.

[29] S. Essig and K. Busch, "Generation of adaptive coordinates and their use in the Fourier Modal Method," *Opt. Express*, vol. 18, pp. 23258-23274, 2010.

[30] V. Liu and S. Fan, "S^4: A free electromagnetic solver for layered periodic structures," *Computer Physics Communications*, vol. 183, pp. 2233-2244, 2012.

[31] K. B. Dossou, L. C. Botten, A. A. Asatryan, B. C. P. Sturmberg, M. A. Byrne, C. G. Poulton, R. C. McPhedran, and C. M. de Sterke, "Modal formulation for diffraction by absorbing photonic crystal slabs," *J. Opt. Soc. Am. A*, vol. 29, pp. 817-831, 2012.

[32] J. P. Berenger, "A perfectly matched layer for the absorption of electromagnetic-waves," *J. Comput. Phys.*, vol. 114, no. 2, pp. 185-200, 1994.

[33] W. C. Chew and W. H. Weedon, "A 3D perfectly matched medium from modified Maxwells equations with stretched coordinates," *Microwave and Optical Technology Letters*, vol. 7, no. 13, pp. 599-604, 1994.

[34] W. P. Huang, C. L. Xu, W. Lui, and K. Yokoyama, "The perfectly matched layer boundary condition for modal analysis of optical waveguides: leaky mode calculations," *IEEE Photon. Technol. Lett.*, vol. 8, no. 5, pp. 652-654, 1996.

[35] H. Derudder, D. De Zutter, and F. Olyslager, "Analysis of waveguide discontinuities using perfectly matched layers," *Electronics Letters*, vol. 34, no. 22, pp. 2138-2140, 1998.

[36] Y. Huang and Y. Y. Lu, "Scattering from periodic arrays of cylinders by Dirichlet-to-Neumann maps," *J. Lightwave Technol.*, vol. 24, pp. 3448-3453, 2006.